JOC Article

Self-Assembled Hemicapsules with Inherent Functionalities: Modeling of a Supramolecular Electrostatic Self-Assembly

Gennady V. Oshovsky, David N. Reinhoudt, and Willem Verboom*

Laboratory of Supramolecular Chemistry and Technology, MESA+ Research Institute for Nanotechnology, University of Twente, P.O. Box 217, 7500 AE Enschede, The Netherlands

w.verboom@utwente.nl

Received June 29, 2006

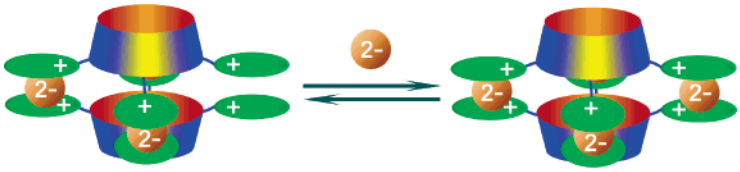

An approach to functional self-assembled hemicapsules is described consisting of the use of multivalent (valency ≥ 4) and divalent components, the functional groups of which have a relatively weak binding affinity. Electrostatic self-assembly of tetrakis(pyridiniummethyl)cavitand hemispheres (H) and doubly charged anions (A) in polar media gives rise to an equilibrium mixture that consists, as detected with ESI-MS, of hemicapsule H_2A_3, capsule H_2A_4, and other ion-pair associates. Fitting ^{1}H NMR data with a model that includes (hemi)capsules and ion-pair associates gave an effective molarity (EM) for the intramolecular assembly of the host (H) with sulfate (A) of 0.19 ± 0.02 M and binding constants of the functional [2 + 3] hemicapsules H_2A_3 and the [2 + 4] capsules H_2A_4 in methanol of 3.25×10^{12} M^{-4} and 3.45×10^{15} M^{-5}, respectively. A substantial amount of the functional [2 + 3] hemicapsules H_2A_3 with respect to [2 + 4] capsules H_2A_4 is present in solution, with ratios of H_2A_3 to H_2A_4 of 5.67−0.43 in the studied concentration range (0.1−25 mM of $[H]_{tot}$). The [2 + 3] hemicapsules H_2A_3 built with sulfate linkers incorporate guests between the closely positioned pyridinium planes.

Introduction

Supramolecular chemistry aims at developing highly complex systems from components interacting through noncovalent intermolecular forces.[1] Self-assembly comprises the spontaneous generation of a well-defined, discrete supramolecular architecture from a given set of components under thermodynamic equilibrium.[2,3] Self-assembly processes driven by *strong* interactions and/or carried out in noncompetitive media exclusively lead to the final product.[4,5] A high binding affinity between receptor and ligand, supported by multivalency,[6] excludes intermediates[4] and provides narcissistic self-sorting.[5] However, in the case of *weak* interactions, especially in the case of self-association in polar competitive media, it is expected that partial assemblies will be present in substantial amounts at equilibrium conditions.

Capsules are an example of complex assemblies.[7] Nowadays, in addition to [1 + 1] capsules[8] and hexameric resorcinarene capsule-like assemblies,[9] [2 + 4] capsules[10−13] attract substantial attention. These capsules contain half-spheres, which are brought together by four linkers (for example, **1**). For the construction of such capsules in solution, quite strong interactions have been used (such as metal−ligand[10,11] or hydrogen bonding[12]).

(1) Lehn, J.-M. *Science* **2002**, *295*, 2400−2403.
(2) Whitesides, G. M.; Grzybowski, B. *Science* **2002**, *295*, 2418−2421.
(3) For reviews on self-assembly, see: (a) Yu, S. Y.; Li, S. H.; Huang, H. P.; Zhang, Z. X.; Jiao, Q.; Shen, H.; Hu, X. X.; Huang, H. *Curr. Org. Chem.* **2005**, *9*, 555−563. (b) Keizer, H. M.; Sijbesma, R. P. *Chem. Soc. Rev.* **2005**, *34*, 226−234. (c) Davis, J. T. *Angew. Chem., Int. Ed.* **2004**, *43*, 668−698. (d) Johnson, D. W.; Raymond, K. N. *Supramol. Chem.* **2001**, *13*, 639−659. (e) Sherrington, D. C.; Taskinen, K. A. *Chem. Soc. Rev.* **2001**, *30*, 83−93. (f) Albrecht, M. *Chem. Rev.* **2001**, *101*, 3457−3497. (g) Leininger, S.; Olenyuk, B.; Stang, P. J. *Chem. Rev.* **2000**, *100*, 853−907. (h) Fujita, M. *Chem. Soc. Rev.* **1998**, *27*, 417−425. (i) Linton, B.; Hamilton, A. D. *Chem. Rev.* **1997**, *97*, 1669−1680.
(4) (a) Pfeil, A.; Lehn, J.-M. *J. Chem. Soc., Chem. Commun.* **1992**, 838−840. (b) ten Cate, M. G. J.; Huskens, J.; Crego-Calama, M.; Reinhoudt, D. N. *Chem.—Eur. J.* **2004**, *10*, 3632−3639.
(5) Taylor, P. N.; Anderson, H. L. *J. Am. Chem. Soc.* **1999**, *121*, 11538−11545.
(6) (a) Badjić, J. D.; Nelson, A.; Cantrill, S. J.; Turnbull, W. B.; Stoddart, J. F. *Acc. Chem. Res.* **2005**, *38*, 723−732. (b) Mulder, A.; Huskens, J.; Reinhoudt, D. N. *Org. Biomol. Chem.* **2004**, *2*, 3409−3424. (c) Mammen, M.; Choi, S. K.; Whitesides, G. M. *Angew. Chem., Int. Ed.* **1998**, *37*, 2755−2794.
(7) (a) Rebek, J. *Angew. Chem., Int. Ed.* **2005**, *44*, 2068−2078. (b) Hof, F.; Craig, S. L.; Nuckolls, C.; Rebek, J. *Angew. Chem., Int. Ed.* **2002**, *41*, 1488−1508. (c) Rudkevich, D. M. *Bull. Chem. Soc. Jpn.* **2002**, *75*, 393−413.

10.1021/jo061344w CCC: $33.50
Published on Web 08/18/2006

SCHEME 1. Equilibrium between [2 + 3] Hemicapsule 2 and [2 + 4] Capsule 1: The Formation of the Hemicapsule−Guest Complexes 3 (A and C are Singly Charged Anions and Cations, Respectively)

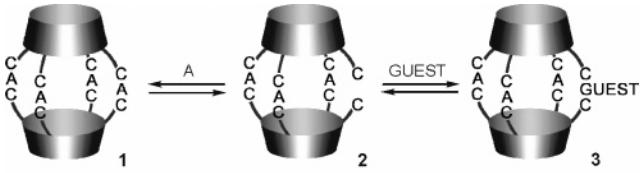

Recently, we reported the presence of functional [2 + 3] hemicapsules in the gas phase, along with novel [2 + 4] capsules based on triple ion interactions.[14] The [2 + 3] hemicapsules **2** have two noncomplexed functionalities in comparison with the [2 + 4] capsules **1**, which enables them to form host−guest complexes **3** (Scheme 1).[14] To the best of our knowledge, these [2 + 3] hemicapsules are the first example of functional hemi-self-assemblies, and they are a new type of self-assembled receptors.[15]

Here we describe a general approach to this type of hemi-self-assemblies, consisting of several multivalent and low-valent components. The multivalent component should have at least four or more binding groups, which are organized on a suitable (non)covalent scaffold, and the low-valent one should have only two valencies, which would allow one to bring the two multivalent components together. The interaction between the multivalent and low-valent components should be relatively weak to avoid exclusive formation of the self-assembly (for example, [2 + 4] capsule **1**). The widely exploited multivalency approach[6] leads to strong self-assemblies, as we recently demonstrated for the formation of [1 + 1] capsules based on four azinium−sulfonate interactions ($K_a > 10^6$ M^{-1}, in methanol).[16]

CHART 1. Tetrakis(pyridiniummethyl)tetramethyl Cavitand Salts

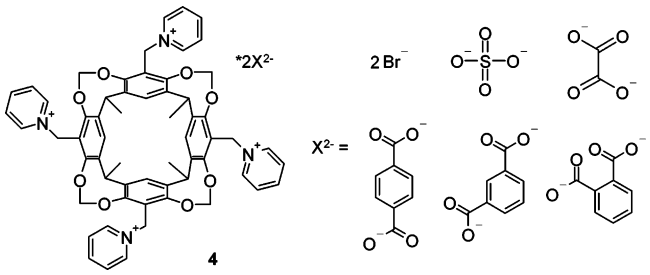

In this study, we used tetrakis(pyridiniummethyl)cavitands **4** as the high-valent component (four valencies organized on a cavitand scaffold) and different doubly charged anions as the low-valent component (two valencies). With electrospray ionization mass spectrometry (ESI-MS), the different assemblies were qualitatively identified. A new model was elaborated, which quantifies all species present in solution and proves the presence of substantial amounts of the functional [2 + 3] hemicapsules with respect to the [2 + 4] capsules, dependent on the concentration. The functionality of the [2 + 3] hemicapsules is demonstrated by its complexation behavior.

Results and Discussion

Synthesis. Salts of tetrakis(pyridiniummethyl)cavitand tetracation **4** with doubly charged anions of different size (sulfate, oxalate, terephthalate, isophthalate, and phthalate) were prepared starting from the tetrabromide[17] **4** × 4Br (Chart 1) using a column loaded with a Dowex anion exchange resin functionalized with the appropriate anion.[18] With this method, all unwanted counterions are removed from the sample, and therefore, it avoids possible by-processes, such as contact ion-pair or triple ion formation with the initial counterion.[19]

A column loaded with Dowex SO_4 was used to prepare *N*-(4-methylbenzyl)pyridinium sulfate **5** as a model compound from the corresponding bromide.

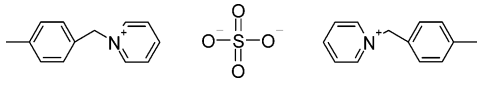

5

^{1}H NMR and ESI-MS Study. It is known that ion pairing between a pyridinium cation and an anion in solution is accompanied by changes of the shifts of the pyridinium

(8) For recent examples of [1 + 1] capsule studies, see: (a) Ajami, D.; Rebek, J. *J. Am. Chem. Soc.* **2006**, *128*, 5314−5315. (b) Ananchenko, G. S.; Udachin, K. A.; Ripmeester, J. A.; Perrier, T.; Coleman, A. W. *Chem.−Eur. J.* **2006**, *12*, 2441−2447. (c) Corbellini, F.; Knegtel, R. M. A.; Grootenhuis, P. D. J.; Crego-Calama, M.; Reinhoudt, D. N. *Chem.−Eur. J.* **2005**, *11*, 298−307. (d) Corbellini, F.; van Leeuwen, F. W. B.; Beijleveld, H.; Kooijman, H.; Spek, A. L.; Verboom, W.; Crego-Calama, M.; Reinhoudt, D. N. *New J. Chem.* **2005**, *29*, 243−248. (e) Kobayashi, K.; Ishii, K.; Yamanaka, M. *Chem.−Eur. J.* **2005**, *11*, 4725−4734. (f) Zadmard, R.; Kraft, A.; Schrader, T.; Linne, U. *Chem.−Eur. J.* **2004**, *10*, 4233−4239. (g) Shivanyuk, A.; Saadioui, M.; Broda, F.; Thondorf, I.; Vysotsky, M. O.; Rissanen, K.; Kolehmainen, E.; Böhmer, V. *Chem.−Eur. J.* **2004**, *10*, 2138−2148. (h) Letzel, M. C.; Decker, B.; Rozhenko, A. B.; Schoeller, W. W.; Mattay, J. *J. Am. Chem. Soc.* **2004**, *126*, 9669−9674. (i) Moon, K.; Kaifer, A. E. *J. Am. Chem. Soc.* **2004**, *126*, 15016−15017.

(9) (a) Dalgarno, S. J.; Tucker, S. A.; Bassil, D. B.; Atwood, J. L. *Science* **2005**, *309*, 2037−2039. (b) Yamanaka, M.; Shivanyuk, A.; Rebek, J. *J. Am. Chem. Soc.* **2004**, *126*, 2939−2943.

(10) (a) Yamanaka, M.; Yamada, Y.; Sei, Y.; Yamaguchi, K.; Kobayashi, K. *J. Am. Chem. Soc.* **2006**, *128*, 1531−1539. (b) Zuccaccia, D.; Pirondini, L.; Pinalli, R.; Dalcanale, E.; Macchioni, A. *J. Am. Chem. Soc.* **2005**, *127*, 7025−7032. (c) Pinalli, R.; Cristini, V.; Sottili, V.; Geremia, S.; Campagnolo, M.; Caneschi, A.; Dalcanale, E. *J. Am. Chem. Soc.* **2004**, *126*, 6516−6517.

(11) Baldini, L.; Ballester, P.; Casnati, A.; Gomila, R. M.; Hunter, C. A.; Sansone, F.; Ungaro, R. *J. Am. Chem. Soc.* **2003**, *125*, 14181−14189.

(12) Kobayashi, K.; Shirasaka, T.; Yamaguchi, K.; Sakamoto, S.; Horn, E.; Furukawa, N. *Chem. Commun.* **2000**, 41−42.

(13) (a) Harrison, R. G.; Burrows, J. L.; Hansen, L. D. *Chem.−Eur. J.* **2005**, *11*, 5881−5888. (b) Harrison, R. G.; Dalley, N. K.; Nazarenko, A. Y. *Chem. Commun.* **2000**, 1387−1388.

(14) Oshovsky, G. V.; Reinhoudt, D. N.; Verboom, W. *J. Am. Chem. Soc.* **2006**, *128*, 5270−5278.

(15) For recent examples of self-assembled receptors, see: (a) Davis, A. V.; Fiedler, D.; Seeber, G.; Zahl, A.; van Eldik, R.; Raymond, K. N. *J. Am. Chem. Soc.* **2006**, *128*, 1324−1333. (b) Tashiro, S.; Tominaga, M.; Yamaguchi, Y.; Kato, K.; Fujita, M. *Angew. Chem., Int. Ed.* **2006**, *45*, 241−244. (c) Kerckhoffs, J. M. C. A.; ten Cate, M. G. J.; Mateos-Timoneda, M. A.; van Leeuwen, F. W. B.; Snellink-Ruel, B.; Spek, A. L.; Kooijman, H.; Crego-Calama, M.; Reinhoudt, D. N. *J. Am. Chem. Soc.* **2005**, *127*, 12697−12708. (d) Ballester, P.; Oliva, A. I.; Costa, A.; Deya, P. M.; Frontera, A.; Gomila, R. M.; Hunter, C. A. *J. Am. Chem. Soc.* **2006**, *128*, 5560−5569. (e) Saur, B.; Scopelliti, R.; Severin, K. *Chem.−Eur. J.* **2006**, *12*, 1058−1066. (f) Roitzsch, M.; Lippert, B. *Angew. Chem., Int. Ed.* **2006**, *45*, 147−150.

(16) Oshovsky, G. V.; Reinhoudt, D. N.; Verboom, W. *Eur. J. Org. Chem.* **2006**, 2810−2816.

(17) Grote Gansey, M. H. B.; Bakker, F. K. G.; Feiters, M. C.; Geurts, H. P. M.; Verboom, W.; Reinhoudt, D. N. *Tetrahedron Lett.* **1998**, *39*, 5447−5450.

(18) Attempts to prepare salts **1** with doubly charged anions by precipitation from an aqueous solution of **1** × 4Br upon addition of excess disodium sulphate, oxalate, terephthalate, isophthalate, or phthalate led to only partial substitution of bromide. The precipitated salts kept up to two bromide anions.

(19) About the importance of ion pairing with initial counterions in electrostatic self-assembly, see ref 16.

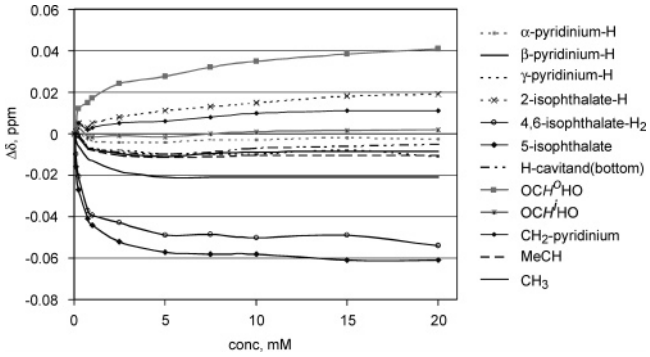

FIGURE 1. ^{1}H NMR shift differences observed upon dilution of **4** × 2isophthalate in methanol-d_4 (with respect to the shifts of **4** × 2isophthalate at 0.05 mM).

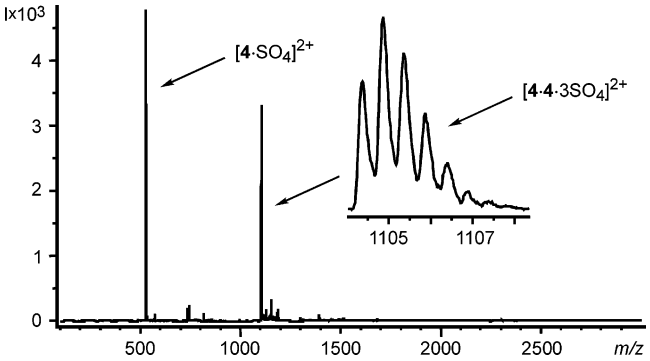

FIGURE 2. Nano ESI-MS continuous flow spectrum of a 5 mM solution[23] of **4** × 2SO$_4$ in methanol (voltages: capillary = 2500 V, orifice 1 and 2 = 1 V, ring lens = 30 V).

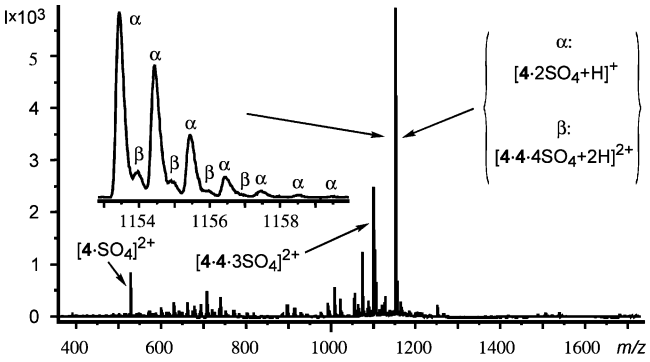

FIGURE 3. Nano ESI-MS continuous flow spectrum of a 5 mM solution of **4** × 2SO$_4$ in methanol containing small additives of formic acid (voltages: capillary = 2500 V, orifice 1 and 2 = 1 V, ring lens = 30 V).

hydrogens in the ^{1}H NMR spectra.[20] Dilution experiments of compounds **4** and **5** in methanol-d_4 displayed changes of all the hydrogens in their ^{1}H NMR spectra. It is interesting to note that depending on the anion the hydrogens of the pyridinium ring experience different ^{1}H NMR shift differences. For example, in the case of **4** × 2SO$_4$, the largest shift difference is observed for the α-pyridinium hydrogen (>0.04 ppm, dilution 20−0.05 mM). However, in the case of isophthalate, the *β*-pyridinium hydrogen shows the larger relative shift difference (∼0.02 ppm, the same concentration range), while the influence of the concentration changes on the shifts of the α-pyridinium hydrogens is negligible. The difference between the sulfate and isophthalate is probably caused by an additional specific influence of the ring currents of the substituted benzene[21] on the pyridinium protons in the ion pairs. Relatively large ^{1}H NMR shifts, indicating the ion pairing, are also observed for the protons of isophthalate (Figure 1).

In the case of compounds **4**, ion pairing can lead to several species depending on the number of ion-paired anions, for example, [**4** × A]$^{2+}$, [**4** × 2A]^0, [**4** × 3A]$^{2-}$, [**4** × 4A]$^{4-}$ (A is doubly charged anion, sulfate, oxalate, terephthalate, isophthalate, and phthalate). These formulas indicate how many pyridinium substituents are ion-paired, but can represent several isomers. Complexes containing two cavitands **4** should possess at least one pyridinium−A−pyridinium linker and can be represented by the next formulas: [**4**$_2$ × A]$^{6+}$, [**4**$_2$ × 2A]$^{4+}$, [**4**$_2$ × 3A]$^{2+}$, [**4**$_2$ × 4A]^0, [**4**$_2$ × 5A]$^{2-}$, etc. These species could present either linear aggregates or (hemi)capsules.

Electrospray ionization mass spectrometry (ESI-MS) allows the easy observation of charged species. A typical mass spectrum of **4** × 2A salts only contains two main signals: [**4**·A]$^{2+}$ and [**4**$_2$·3A]$^{2+}$ (for example, A = SO_4^{2-}, Figure 2).[22]

The complex represented by the [**4**·SO$_4$]$^{2+}$ signal at *m*/*z* 528 is sensitive to changes of the ring lens voltage (for example, it completely disappears when the voltage is 40 V). Upon increase of the orifice voltage, it can lose up to three pyridines. Similarly to the in-source voltage-induced fragmentation experiments,[14,16] it indicates that a sulfate anion stabilizes one pyridinium moiety by ion pairing, while the other unstabilized pyridiniums are cleaved off. The complex represented by the [**4**$_2$·3SO$_4$]$^{2+}$ signal at *m*/*z* 1105 is more stable against ring lens voltage changes, similarly to the signals of the hemicapsules compared with simple ion-pair associates.[14]

The signals of the negatively charged [**4**·3A]$^{2-}$ complexes are observed in the negative ion mode ESI-MS spectra.

The expected species [**4**·2A]^0 and [**4**$_2$·4A]^0 are electrically neutral and, hence, are invisible in both positive and negative ion mode ESI-MS spectra. However, addition of a small amount of formic acid allowed the observation of these species due to protonation. For example, in the spectrum of a 5 mM solution[23] of **4** × 2SO$_4$, a new very intensive signal appeared at *m*/*z* 1153 (Figure 3) corresponding to [**4**·2SO$_4$ + H]$^+$. It is superimposed with [**4**$_2$·4SO$_4$ + 2H$^+$]$^{2+}$. A small signal of [**4**$_2$·4SO$_4$ + H$^+$]$^+$ at *m*/*z* 2307 is also present in the spectrum. Due to the different protonation efficiency of pyridinium−sulfonate and pyridinium−sulfonate−pyridinium contact ion pairs (the first one contains an easily protonable O$^-$), the relative intensity of the species cannot be used even for a qualitative estimation of the relative concentration of these species in solution.

ESI-MS (normal and nano) detects a number of associates, such as [**4** × A]$^{2+}$, [**4** × 2A]^0, [**4** × 3A]$^{2-}$, [**4**$_2$ × 3A]$^{2+}$, and [**4**$_2$ × 4A]^0 containing one or two tetrakis(pyridiniummethyl)-tetramethyl cavitands with several anions. The [**4** × A]$^{2+}$, [**4** × 2A]^0, and [**4** × 3A]$^{2-}$ associates correspond to simple ion-paired species. In accordance with the stoichiometry, the [**4**$_2$ × 3A]$^{2+}$

(20) Chuck, R. J.; Randall, E. W. *Spectrochim. Acta* **1966**, *22*, 221−226.

(21) Wannere, C. S.; Schleyer, P. v. R. *Org. Lett.* **2003**, *5*, 605−608.

(22) To keep a clear difference between compounds and ESI-MS signals, they are represented with the use of × and · symbols (for example, **4** × 2SO$_4$ and [**4**$_2$·3SO$_4$]$^{2+}$), respectively.

(23) Nano ESI-MS continuous flow experiments of a 25 mM solution of **3** × 2SO$_4$ were practically impossible due to the very easy stoppering of the nano needle.

SCHEME 2. Ion Pairing between a Singly Charged Cation and a Doubly Charged Anion

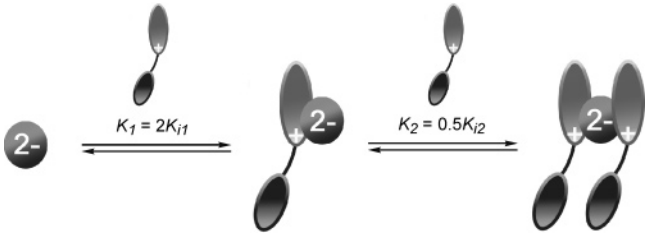

SCHEME 3. Formation of Multiple Associates of Tetrapyridinium Cation 4 with a Doubly Charged Small Anion

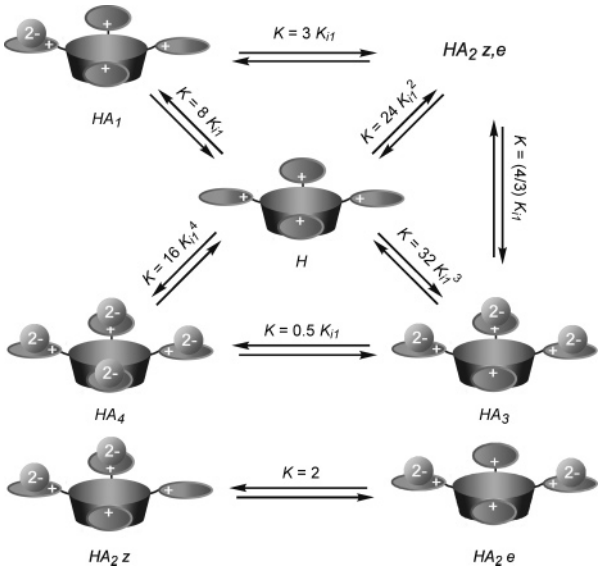

and $[\mathbf{4}_2 \times 4A]^0$ associates could correspond to nonspecific associates or (hemi)capsules. However, due to the higher voltage stability of $[\mathbf{4}_2 \times 3A]^{2+}$ and the relatively low ability of $[\mathbf{4}_2 \times 4A]^0$ to be protonated, it may be concluded that a substantial part of these species correspond to the (hemi)capsules H_2A_3 and H_2A_4. To validate this conclusion and to determine the composition of the equilibrium mixture in solution, the equilibrium was described with a model.

Modeling of the Composition of the Equilibrium Mixture. The association processes based on anion−pyridinium interactions are relatively weak, in comparison with metal−ligand self-assembly, and as a consequence give rise to the presence of a number of intermediates containing one or two tetrakis(pyridiniummethyl)tetramethyl cavitands **4** with one or more anions. Since the species that could correspond to complexes containing more than two cavitands **4** have a negligibly low intensity in the ESI-MS spectrum, their value in the equilibrium will be unimportant at the concentrations studied. To quantify the extent to which the associates are present in the equilibrium at a given concentration, a model was developed as depicted in Schemes 2−5. Tetrakis(pyridiniummethyl)tetramethyl cavitand **4** looks like an open flower in the most energetically favorable structure[14] and, therefore, is schematically represented as such. Nonspecific dimers containing two tetrakis(pyridiniummethyl)-tetramethyl cavitands **4** with two or more anions (for example, $HA_2 \times HA_1$, Figure 4) are relatively weaker than the assemblies (for example, H_2A_3, Figure 4), and hence, they are not included in the models (H = host, tetrakis(pyridiniummethyl)tetramethyl

SCHEME 4. Formation of H_2A

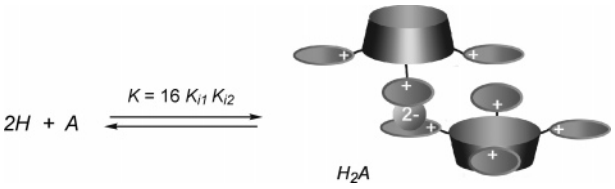

SCHEME 5. Association Processes Leading to Hemicapsules and Capsules, Based on Pyridinium Cavitands 4× 2A and Small Doubly Charged Anions

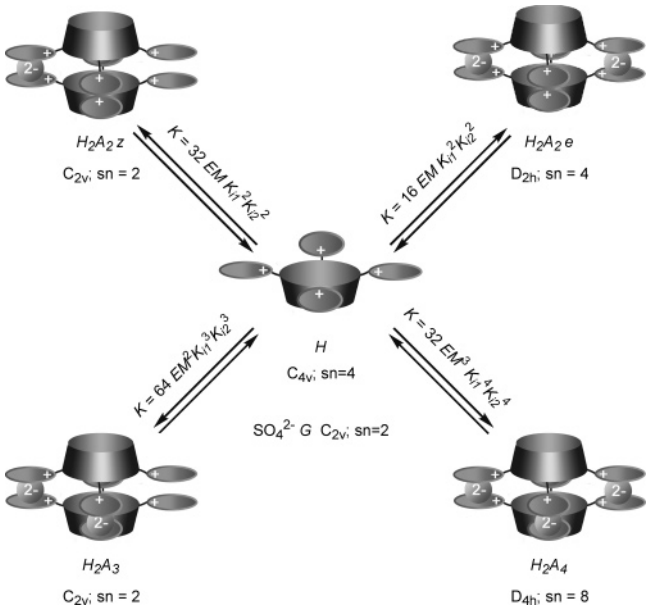

cavitand **4**; A = anion, sulfate). The validity of this approximation is described under the nonspecific dimers section (vide infra).

The intrinsic binding constants of the interaction of pyridinium with sulfate were determined using ^{1}H NMR dilution data of the reference compound **5** ($K_1 = 560 \pm 30$ M^{-1} and $K_2 = 20 \pm 2$ M^{-1}). The relationship between the binding constants and the intrinsic binding constants is shown in Scheme 2.[24] K_{i1} and K_{i2} are the intrinsic binding constants representing the interaction of pyridinium with a doubly charged anion and of the resulting contact ion pair with another pyridinium, respectively. Using these equations,[25] $K_{i1} = 280$ M^{-1} and $K_{i2} = 40$ M^{-1}. The difference between the values for the 1:1 and 1:2 complexation process shows that the first ion pairing strongly decreases the ability of the sulfate to form the second ion-pair pattern.

The association constants of complexes of tetrakis(pyridiniummethyl)tetramethyl cavitands **4** with one, two, three, or four small anions contain the intrinsic binding constant between

(24) The coefficient 2 (and not 4) for the first step of the complexation of the sulfate dianion with the pyridinium cation (K_{i1}) is chosen because it is known from X-ray crystal structures of (solvated) SO_4^{2-} that, in general, the sulfur−oxygen bonds are not equivalent, with a difference in the length of up to 0.027 Å: (a) Larson, A. C. *Acta Crystallogr.* **1965**, *18*, 717−724. (b) Szafran, M.; Jaskólski, M.; Kowalczyk, I.; Dega-Szafran, Z. *J. Mol. Struct.* **1998**, *448*, 77−89. The solvation shell covers SO_4^{2-} both in solution and in the gas phase, (c) Blades, A. T.; Kebarle, P. *J. Am. Chem. Soc.* **1994**, *116*, 10761−10766, and is supposed to cause distortions of the symmetric resonance tetrahedral structure of the anion.

(25) Connors, K. A. *Binding Constants: The Measurement of Molecular Complex Stability*; Wiley-Interscience: New York, 1987.

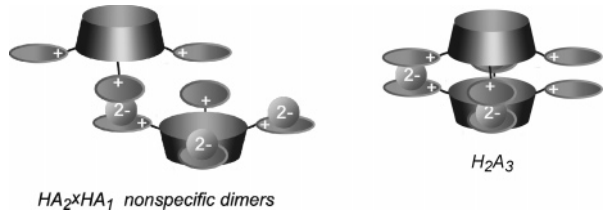

FIGURE 4. An example of nonspecific dimer $HA_2 \times HA_1$ in comparison with [2 + 3] hemicapsule H_2A_3.

pyridinium and the anion and an additional statistic coefficient[25] (Scheme 3). A small anion, sulfate, was chosen to exclude intramolecular formation of pyridinium−anion−pyridinium associates. The HA_2 complex has two isomers z and e ($K = 16K_{i1}^2$ and $8K_{i1}^2$, respectively) depending on whether the neighboring or opposite pyridinium substituents are ion-paired (the chosen nomenclature is arbitrary, related to z = zusammen and e = entgegen). The ion pairing can take place on either side of the pyridinium plane because the isomers can be transformed into one another by rotation around the CH_2−pyridinium bond; only one of the isomers (complexes above the pyridinium plane) is shown.

The formation of a complex, which contains two tetrakis-(pyridiniummethyl)cavitands **4** and one anion, is described by a binding constant that incorporates K_{i1} and K_{i2} (Scheme 4).

The consideration of the binding constants of the formation of hemicapsules and capsules of **4** × 2A in solution is based on the self-assembly model proposed by Ercolani (eq 1).[26,27] K_s is the constant of the assembly formation, σ_{sa} is the symmetry factor of the self-assembly equilibrium (eq 2), and K_i is the intrinsic binding constant. The number *n* represents the number of interactions, and *m* describes the number of independent intramolecular noncovalent "loops" that give the self-assembly. The tendency to form intramolecular complexes is expressed in terms of effective molarity (EM) defined as K_{intra}/K_{inter}.[26−28] The averaged EM value is used to describe the formation of intramolecular loops.[26] The coefficients σ_1, σ_2, and σ_s in eq 2 are symmetry numbers of the components of an assembly (1 and 2) and the assembly itself, respectively. The numbers *a* and *b* describe the number of components 1 and 2 in the assembly, respectively. The resulting equations, point groups, and symmetry numbers of the different assemblies are depicted in Scheme 5. The model was designed as noncooperative since the pyridinium substituents in tetrakis(pyridiniummethyl)tetramethyl cavitand **4** are located quite far away from each other and experience no intramolecular interaction.[27]

$$K_s = \sigma_{sa} K_i^n \mathrm{EM}^m \quad (1)$$

$$\sigma_{sa} = \sigma_1^a \sigma_2^b / \sigma_s \quad (2)$$

Maple provides a solution of the set of equations, which describes the composition of the equilibrium mixture at different concentrations. The values for the intrinsic binding constant were taken from experiments with reference compound **5**: $K_{i1} = 280$ M^{-1} and $K_{i2} = 40$ M^{-1}. Fitting the calculated values (Figure 5) with the results of the ^{1}H NMR dilution experiments of **4** × $2SO_4$ yielded an EM value of 0.19 ± 0.02 M. The binding

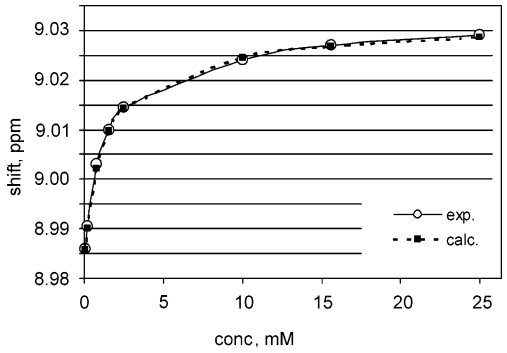

FIGURE 5. Fitting ^{1}H NMR dilution data of **4** × $2SO_4$ in methanol-d_4 to the model.

TABLE 1. Binding Constants of the Formation of the Capsules, Hemicapsules, and Ion-Paired Associates Calculated Using the Model (EM = 0.19 M, K_{i1} = 280 M^{-1}, K_{i2} = 40 M^{-1})

no.	complexes	binding constants[a]
1	$[HA_1]$	2.24×10^3 M^{-1}
2	$[HA_2\,z]$	1.25×10^6 M^{-2}
3	$[HA_2\,e]$	6.27×10^5 M^{-2}
4	$[HA_3]$	7.02×10^8 M^{-3}
5	$[HA_4]$	9.83×10^{10} M^{-4}
6	$[H_2A_1]$	1.79×10^5 M^{-2}
7	$[H_2A_2\,z]$	7.63×10^8 M^{-3}
8	$[H_2A_2\,e]$	3.81×10^8 M^{-3}
9	$[H_2A_3]$	3.25×10^{12} M^{-4}
10	$[H_2A_4]$	3.45×10^{15} M^{-5}

[a] The error is <7%.

constants for the species considered in the model are summarized in Table 1.

The composition of the equilibrium mixture with a set of concentrations between 0.1 and 25 mM is given in the Supporting Information. The formation of reasonable amounts of [2 + 3] hemicapsules H_2A_3 is possible due to the use of relatively weak interactions. For example, the K_a value of [2 + 4] capsule formation is 3.45×10^{15} M^{-5} (Table 1), which is 18 orders of magnitude lower than that reported for calix[4]arene [2 + 4] capsules based on Zn−porphyrin + DABCO interactions (6.3×10^{33} M^{-5}),[11] where no hemi-self-assemblies have been detected.

The ratio between the functional [2 + 3] hemicapsule H_2A_3 and the [2 + 4] capsule H_2A_4 depends on the concentration of **4** × $2SO_4$ (Figure 6). At lower concentrations, the [2 + 3] hemicapsule H_2A_3 dominates (for example, the ratio H_2A_3/H_2A_4 is 5.67 in a 0.1 mM solution of **4** × $2SO_4$). However, the concentration of the [2 + 4] capsule H_2A_4 grows faster than that of the [2 + 3] hemicapsule H_2A_3 (Figure 6). At a 25 mM concentration of **4** × $2SO_4$, there is about 2.3 times more [2 + 4] capsule H_2A_4 than [2 + 3] hemicapsule H_2A_3 in the solution.

The different species, HA_1, H_2A_3, HA_2 (z+e), HA_3, and H_2A_4, which are present in the equilibrium mixture in reasonable amounts according to the model, were also detected by ESI-MS spectrometry (vide supra).[29] Figure 7 shows the distribution of tetrakis(pyridiniummethyl)cavitand **4**, the multivalent com-

(26) Ercolani, G. *J. Phys. Chem. B* **2003**, *107*, 5052−5057.
(27) Ercolani, G. *J. Am. Chem. Soc.* **2003**, *125*, 16097−16103.
(28) Galli, C.; Mandolini, L. *Eur. J. Org. Chem.* **2000**, 3117−3125.

(29) Due to a different volatility, charge, protonation ability, stability, etc. of the species, the intensity of the signals in the mass spectra is dependent on many unknowns and, consequently, gives only qualitative information. For details, see: Oshovsky, G. V.; Verboom, W.; Fokkens, R. H.; Reinhoudt, D. N. *Chem.—Eur. J.* **2004**, *10*, 2739−2748.

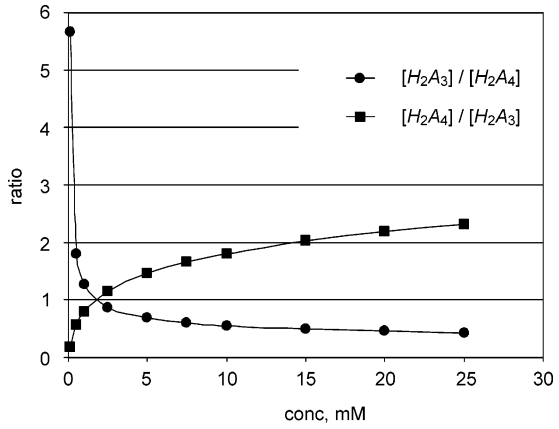

FIGURE 6. Ratios between the functional [2 + 3] hemicapsule H_2A_3 and the [2 + 4] capsule H_2A_4.

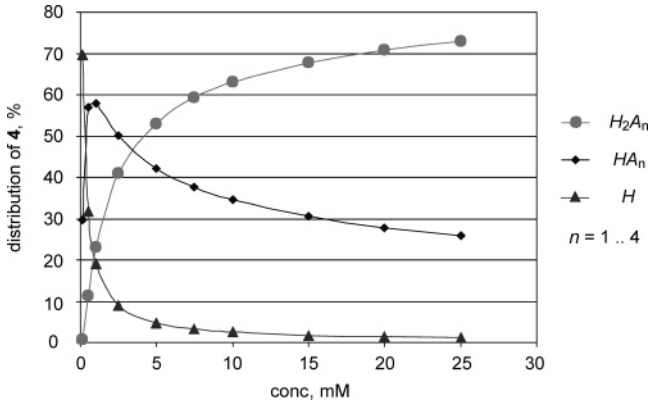

FIGURE 7. Distribution of tetrakis(pyridiniummethyl)cavitand **4** (H) between different groups of complexes in solution.

SCHEME 6. Equilibrium between the Nonspecific Dimers $HA_2 \times HA_1$ and the [2 + 3] Hemicapsule H_2A_3 (the Schematic Structures are Shown in Figure 4)

$$HA_2 \times HA_1 \text{ nonspecific dimers} \underset{}{\overset{K = (2/3)\, EM^2 K_{i2}^2}{\rightleftharpoons}} H_2A_3$$

ponent H of the self-assembly, between complexes containing one H (HA_1, HA_2 z, HA_2 e, HA_3, HA_4) and two H's (H_2A_1, H_2A_2 z, H_2A_2 e, H_2A_3, H_2A_4). It demonstrates that at low concentration of **4** × $2SO_4$ H and HA_n ($n = 1-4$) species dominate. Higher associates H_2A_n ($n = 1-4$), especially the hemicapsule H_2A_3 and the capsule H_2A_4, are the most sensitive to concentration changes, and in a 25 mM solution of **4** × $2SO_4$, they consume about 73% of it.

Nonspecific Dimers. The model neglects the formation of nonspecific dimers $HA_n \times HA_m$ ($n + m = 2-7$). For example, one of the isomers of nonspecific dimers $HA_2 \times HA_1$ is shown in Figure 4. The binding constant of the dimers $HA_2 \times HA_1$ (as a mixture of isomers) can be treated as a product of the interaction of HA_1 ($K = 8K_{i1}$) with HA_2 z, e ($K = 24K_{i1}^2$). This interaction is characterized by $K = 0.5\ K_{i2}$ (0.5 is the statistic coefficient): $K_{HA_2 \times HA_1} = 96K_{i1}^3K_{i2}$. The binding constant $K_{H_2A_3}$ of the formation of the [2 + 3] hemicapsule H_2A_3 is $64 \times EM^2K_{i1}^3K_{i2}^3$ (vide supra). It allows one to determine the equilibrium constant for the process shown in Scheme 6 ($K = K_{H_2A_3}/K_{HA_2 \times HA_1}$).

In the case of the association of compounds **4** × $2SO_4$ in solution, $K_{i2} = 40\ M^{-1}$ and EM = 0.19 M, hence the equilibrium

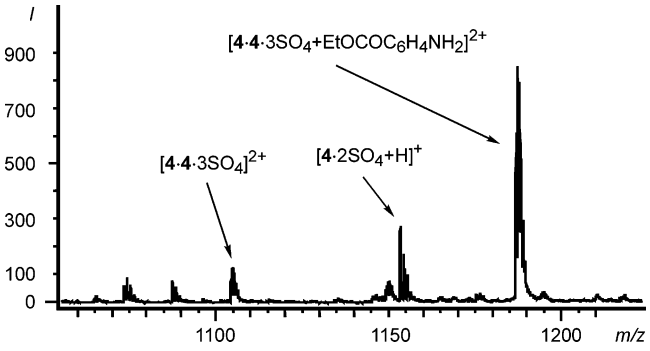

FIGURE 8. Nano ESI-MS continuous flow spectrum of a 5 mM[23] solution of **4** × $2SO_4$ and a 15 mM solution of ethyl 4-aminobenzoate in methanol (voltages: capillary = 2500 V, orifice 1 and 2 = 1 V, ring lens = 10 V).

constant K of the process described in Scheme 6 is 38.5. It means that the concentration of the [2 + 3] hemicapsule H_2A_3 is 38.5 times higher than that of the unspecific dimers $HA_2 \times HA_1$, which allows one to neglect them to give a realistic representation of the dynamic equilibrium. In general, this approach works excellently if the modeled equilibria (vide supra) are characterized by similar and higher binding constants and EM (namely, $K_{i2} \geq 40\ M^{-1}$ and EM ≥ 0.19 M). In addition, this approach can give useful information for even weaker interactions. For example, in the case of a hypothetical process, characterized by $K_{i2} = 20\ M^{-1}$ and EM = 0.19 M, the concentration of the [2 + 3] hemicapsule is an order of magnitude higher than that of nonspecific dimers. However, in the case of $K_{i2} = 10\ M^{-1}$ and EM = 0.19 M, the ratio [2 + 3] hemicapsule/nonspecific dimers is only 2.5, and consequently, these noncapsule associates become important participants of the equilibrium mixture.

Host−Guest Studies. Hemicapsules based on pyridinium−anion−pyridinium triple ion interactions can form complexes with electron-rich aromatic compounds.[14] A similar behavior was observed for the capsules built with doubly charged anions. Upon addition of the methyl and ethyl esters of 4-aminobenzoic acid, 4-iodophenol, and 4-iodoaniline to a methanolic solution of **4** × $2SO_4$ changes of the shifts of the α,β,γ-pyridinium protons were observed (up to 0.3 ppm) in the ^{1}H NMR spectra. In the ESI-MS spectrum of a solution of **4** × $2SO_4$, significant changes took place upon guest addition (Figure 8). For example, an intensive signal at m/z 1187 corresponding to [$\mathbf{4}_2$·$3SO_4$ + ethyl 4-aminobenzoate]$^{2+}$ has appeared, while the intensity of the [$\mathbf{4}_2$·$3SO_4$]$^{2+}$ signal at m/z 1105 was significantly decreased. Several multiple charged signals corresponding to *two* tetrakis(pyridiniummethyl)tetramethyl cavitands **4**, 1−$3SO_4^{2-}$, and 1−3 guest molecules are also present. It should be noted that no complexes of the guests with a *single* molecule of **4** (and **4** × nSO_4^{2-}, $n = 0-4$) are observed. These results indicate that the complexation of the guests takes place between the two pyridiniums of the hemicapsule [$\mathbf{4}_2$·$2SO_4$]$^{2+}$, analogous to the triple-ion-based hemicapsules.[14] It is notorious that in the case of large anions, such as iso- and terephthalate, no such guest complexation was observed either by ^{1}H NMR spectroscopy or ESI-MS. Apparently, in this case, the distance between the pyridiniums is already too large to provide an effective complexation.

Complexation of the guest within the [2 + 4] capsule can be excluded in methanol due to the absence of (large) ^{1}H NMR shifts of the methyl protons of methyl and ethyl 4-amino-

benzoate guests. For a comparison, see the complexation in water (vide infra) and the large ^{1}H NMR shift changes of hydrogens of organic guests induced by complexation in the cavity of the cavitand.[30]

In water, the formation of self-assemblies based on electrostatic interactions is strongly suppressed. However, cavitands have a hydrophobic cavity, in which organic molecules can be complexed, driven by hydrophobic interactions. Sherman et al. have reported the recognition of small organic molecules, such as ethyl acetate, acetone, benzene, and acetonitrile, in water by a cavitand solubilized with four phosphoric acid groups at the bottom rim.[31] Middel et al. described the complexation of phenol, cresol, and benzene by water-soluble cavitands.[32]

Only cavitands **4** × 4Br, **4** × 2SO$_4$, and **4** × 2Oxalate show a moderate solubility in water (>5 mM/L). Titration of aqueous solutions of organic molecules by **3** × 4Br, **4** × 2SO$_4$, and **4** × 2Oxalate indicates a general trend pointing out the similarity of the host−guest behavior between the previously studied cavitands and the new ones. Acetone, acetonitrile, and ethyl acetate are complexed by host **4** × 4Br with binding constants of 30 ± 7, 60 ± 10, and 420 ± 35 M^{-1} in neutral aqueous solution. Compounds **4** × 2SO$_4$ and **4** × 2Oxalate show a similar binding affinity. The methyl and ethyl esters of 4-aminobenzoic acid form complexes with **4** × 2SO$_4$ with K_a values of 680 ± 22 and 640 ± 30 M^{-1}, respectively. The complexation is accompanied by a large ^{1}H NMR shift of the methyl group of the esters (more than 1 ppm).

Conclusions

This study clearly shows that weak electrostatic interactions between multi- and low-valent components (valencies are ≥4 and 2, respectively) give rise to the formation of defined (hemi-) self-assemblies. In the case of the model system, tetrakis-(pyridiniummethyl)tetramethyl cavitand disulfate, that self-assembles due to pyridinium−sulfate interactions, substantial amounts of hemicapsules H_2A_3 are present, dependent on the concentration.

ESI-MS gives qualitative information about the composition of the equilibrium mixture. A newly developed model, which describes the equilibrium, quantifies the composition of the mixture at different concentrations based on ^{1}H NMR dilution data of **4** × 2SO$_4$ and provides an effective molarity (EM) of the intramolecular processes (0.19 ± 0.02 M) and binding constants of the functional [2 + 3] hemicapsules H_2A_3 and the [2 + 4] capsules H_2A_4 in methanol of 3.25 × 10^{12} M^{-4} and 3.45 × 10^{15} M^{-5}, respectively. The [2 + 3] hemicapsules H_2A_3 built with small sulfate linkers incorporate guests between the closely positioned pyridinium planes.

We feel that the predicting value of the model and its general applicability to other self-assembly processes makes it valuable for all practitioners in the field.

Experimental Section

Determination of Binding Constants. EM values of the capsule formation (compound **4** with sulfate) were determined by nonlinear fitting of experimental data obtained by ^{1}H NMR titration experiments with calculated values (equations 3−16; $[H]_{tot}$ and $[A]_{tot}$ are total concentrations of the cation and doubly charged anions, respectively; K_{i1} and K_{i2} are intrinsic binding constants of pyridinium with sulfate determined using reference compound **5**; [H] and [A] are concentrations of the unbound cation and anion, respectively; [HA_1], [HA_2z], [HA_2e], [HA_3], [HA_4], [H_2A_1], [H_2A_2z], [H_2A_2e], [H_2A_3], and [H_2A_4] are the equilibrium concentrations of different complexes in solution; δ_{obs} = calculated shift of the α-pyridinium protons in the equilibrium; δ_H and δ_{HA} are the shifts of the α-pyridinium protons of unbound pyridinium cation and ion-paired pyridinium, respectively). The numerical solution of the system of eqs 1−14 was calculated using Maple 8 software. The nonlinear fitting of calculated to experimental data (EM, δ_H, and δ_{HA}) was carried out by the grid method.[33]

$$[A]_{tot} = 2[H]_{tot} \tag{3}$$

$$[HA_1] = 8K_{i1}[H][A] \tag{4}$$

$$[HA_2z] = 16K_{i1}^2[H][A]^2 \tag{5}$$

$$[HA_2e] = 8K_{i1}^2[H][A]^2 \tag{6}$$

$$[HA_3] = 32K_{i1}^3[H][A]^3 \tag{7}$$

$$[HA_4] = 16K_{i1}^4[H][A]^4 \tag{8}$$

$$[H_2A_1] = 16K_{i1}K_{i2}[H]^2[A] \tag{9}$$

$$[H_2A_2z] = 32K_{i1}^2K_{i2}^2EM[H]^2[A]^2 \tag{10}$$

$$[H_2A_2e] = 16K_{i1}^2K_{i2}^2EM[H]^2[A]^2 \tag{11}$$

$$[H_2A_3] = 64K_{i1}^3K_{i2}^3EM^2[H]^2[A]^3 \tag{12}$$

$$[H_2A_4] = 32K_{i1}^4K_{i2}^4EM^3[H]^2[A]^4 \tag{13}$$

$$[H]_{tot} = [H] + [HA_1] + [HA_2z] + [HA_2e] + [HA_3] + [HA_4] + 2([H_2A_1] + [H_2A_2z] + [H_2A_2e] + [H_2A_3] + [H_2A_4]) \tag{14}$$

$$[A]_{tot} = [A] + [HA_1] + [H_2A_1] + 2([HA_2z] + [HA_2e] + [H_2A_2z] + [H_2A_2e]) + 3([HA_3] + [H_2A_3]) + 4([HA_4] + [H_2A_4]) \tag{15}$$

(30) Oshovsky, G. V.; Verboom, W.; Reinhoudt, D. N. *Collect. Czech. Chem. Commun.* **2004**, *69*, 1137−1148.
(31) Gui, X.; Sherman, J. C. *Chem. Commun.* **2001**, 2680−2681.
(32) Middel, O.; Verboom, W.; Reinhoudt, D. N. *Eur. J. Org. Chem.* **2002**, 2587−2597.
(33) Isotani, S.; Fujii, A. T. *Comput. Phys. Commun.* **2003**, *151*, 1−7.

$$\delta_{obs} = \delta_H \frac{4([H] + [H_2A_2z] + [H_2A_2e]) + 2([HA_2z] + [HA_2e] + [H_2A_3])}{4[H]_{tot}} + \delta_H \frac{[HA_3] + 3[HA_1] + 6[H_2A]}{4[H]_{tot}} + \delta_{HG} \frac{[HA_1] + 3[HA_3] + 6[H_2A_3] + 8[H_2A_4]}{4[H]_{tot}} + \delta_{HG} \frac{2([HA_2z] + [HA_2e] + [H_2A_1]) + 4([HA_4] + [H_2A_2z] + [H_2A_2e])}{4[H]_{tot}} \quad (16)$$

ESI-MS. In the standard mode, the solutions were introduced at a flow rate of 12.5 μL/min. In the continuous nanoflow mode, the solutions were introduced with pressure (the flow rate set in the syringe pump was up to 400 nL/min) into fused silica PicoTip emitters. The data were accumulated in the mass range of 230−4000 *m*/*z* for 2 min. The standard spray conditions, unless otherwise specified include the following: capillary voltage = 2500 V, ring lens voltage = 30 V, orifice 1 voltage = 2 V, orifice 2 voltage = 2 V, orifice 1 temperature = 60 °C, temperature in the desolvation chamber = 120 °C, drying gas flow = 0.1−0.5 L/min, nebulizing gas flow = 0.5 L/min. For the characterization of compounds **4**, the most intensive signals of the isotopic pattern observed are shown. For the host−guest studies, guest concentrations varying from 1.5 to 50 mM in methanol were used.

General Procedure for Ion Exchange. (1) Column Preparation. Dowex anion exchange resin (~150 mL) was washed with methanol (1 L) and placed into a column (*d* = 25 mL), which had a small piece of wool above the stopcock at the bottom of the column. The column was flushed under pressure by methanol (1 L) and Q-water (2 L). Subsequently, it was washed by an aqueous solution of NaOH (1 N, 400 mL, mainly without pressure) and Q-water (1.5 L, with pressure). It was followed by washing with an aqueous solution of the salt chosen (mainly without pressure; 2 L of 0.2 N solutions of sodium sulfate, sodium oxalate, sodium phthalate, sodium isophthalate, and sodium terephthalate in water were used). To remove the excess salt, the column was washed with Q-water (2.5 L) and flushed with MeOH (300−500 mL, with pressure).

(2) Ion Exchange. A solution of compound **4** × 4Br (400 mg) in methanol (20 mL) was flushed into the Dowex anion column without pressure. The column was washed with methanol (200 mL). The methanol solution was evaporated to dryness under vacuum *without heating* to give the **4** × 2Anions in quantitative yields. For the analytical and spectroscopic data of the different salts, see the Supporting Information.

Acknowledgment. The authors warmly thank Prof. Dr. N. M. M. Nibbering for the fruitful discussions on the mass spectrometric part. We are grateful to the Council for Chemical Sciences of The Netherlands Organization for Scientific Research (CW-NWO) for financial support.

Supporting Information Available: Equilibrium concentrations of the capsules, hemicapsules, and ion-paired associates depending on the concentration of the initial salt calculated using the model, general part of the Experimental Section, analytical and spectroscopic data, and copies of the ^{1}H NMR spectra of the different cavitand salts. This material is available free of charge via the Internet at http://pubs.acs.org.

JO061344W